Electric Power Systems Research 207 (2022) 107823

Contents lists available at ScienceDirect

Electric Power Systems Research

journal homepage: www.elsevier.com/locate/epsr

Dynamically adaptive method for under frequency load shedding protection scheme reconfiguration

Tomislav Baškarad [a], Ninoslav Holjevac [a,*], Igor Kuzle [a], Igor Ivanković [b]

[a] University of Zagreb Faculty of Electrical Engineering and Computing, Croatia
[b] Croatian transmission system operator HOPS, Zagreb, Croatia

ARTICLE INFO

Keywords:
Frequency response
Frequency nadir
UFLS
ROCOF relay

ABSTRACT

The increased integration of the new generation technologies into the electric power system (EPS) which are mainly inverter-based changes its characteristics. The main issue that arises is the appearance of faster frequency dynamics that are caused by production connected through inverters. This leads to the need for changing conventional under-frequency load shedding (UFLS) schemes because, in cases of high dynamics of frequency change, conventional UFLS algorithms are not able to stop initial frequency drop and prevent power system collapse. This paper proposes reconfiguration method for conventional strategies transforming their response from static and inflexible to a dynamic and adaptive one. The focus of the paper is the proposed method for dynamical change of UFLS stage thresholds to minimize the number of activated UFLS stages during a particular disturbance event and therefore enable more efficient response of the system to further disturbances. The method effectiveness was demonstrated on a multi-machine power system model consisting of various generation technologies.

1. Introduction

The characteristics of the conventional bulk electric power system are significantly changed due to increased renewable energy sources (RES) integration. The main difference is manifested in the much faster dynamics of frequency change caused by the reduced inertia of the EPS. Inertia becomes time variable and dependent on energy mix of generators in operation during the day. In such low-inertia conditions, the frequency decline during the loss of generation (LOG) events is faster [1] and the probability of activation of under-frequency load shedding protection schemes (UFLS) increases in order to maintain system frequency stability. UFLS is one of the basic protection measures of the transmission system operators (TSO) to maintain the system stability and prevent possible black-outs due to a large frequency deviation. The conventional basic principle is to disconnect a pre-determined part of the consumption, usually divided into several stages with activation triggers with frequency drop below the set value [2]. However, in the cases of high dynamics of frequency change manifested particularly in small time window after the disturbance, conventional UFLS algorithms based solely on frequency deviation are not able to stop further frequency drop and prevent power system collapse. Therefore, a need to improve and adapt conventional UFLS algorithms to the new conditions in the EPS is visible. In view of a typical characteristic of modern smart power systems defined with potentially high values of ROCOF [3] (rate-of-change-of-frequency) during normal system operation the unwanted relay operation or UFLS activation caused by it can lead to even larger problems due to the additional and cascading LOG. Furthermore, these problems can be caused by false loss-of-mains (LOM) relay activation [4] that can happen due to load connection/disconnection, transient phenomena, or any fault in the network. These phenomena lead many power systems operators to adjust the ROCOF withstand capability threshold like the Irish and UK TSOs [5] which have increased the ROCOF threshold values from 0.5 Hz/s to 1 Hz/s. Also, new key performance indices (KPI) have to be defined and calculated in order to prepare automatic reaction of relay and control protection systems [6]. A connection is observed between the ROCOF relays and the UFLS protection; the higher the number of activated generator ROCOF relays during a disturbance in the system, the greater the LOG in the system and thus the greater burden on the UFLS protection. The basic idea of this paper is to develop an algorithm that will combine the signal of an individual generator ROCOF relays and conventional UFLS protection system to propose a new adaptive UFLS protection scheme (Special

* Corresponding author.
E-mail address: ninoslav.holjevac@fer.hr (N. Holjevac).

https://doi.org/10.1016/j.epsr.2022.107823
Received 29 April 2021; Received in revised form 14 January 2022; Accepted 17 January 2022

Protection Schemes) that can reduce the total amount of shed and draw its amount close to the theoretical minimum.

1.1. Literature survey

The term adaptive UFLS technique is not a new one and can be found in the literature. As presented in [7], adaptive UFLS techniques can be divided into several groups depending on the principle on which they are based on: event-based, response-based, ROCOF-based and adaptive with frequency prediction. The proposed technique in this paper is based on the combination of two mentioned groups: ROCOF-based with the inclusion of frequency prediction adaptation.

Several papers propose different adaptive techniques that depend on frequency prediction. The work done in [8] proposes a method that adjusts the UFLS settings based on the predicted frequency minimum f_{nadir}, but governor turbine controls, which significantly affects f_{nadir} and the moment when it will happen, were not taken into account when predicting the frequency minimum. The paper [9] takes into account the turbine governor controls when forecasting the frequency minimum, but this method can be only applied to the single-machine power system. The method presented in [10] adjusts UFLS settings according to the predicted power deficit in the system but this prediction of the power deficit is done off-line and is based on the historical data and probability density functions which means that it has limited adaptability. Methods described in papers [11, 12] and [13] aim to achieve optimal UFLS settings but use models for predicting frequency trajectory and f_{nadir} that are constrained to utilization of low-order turbine models making them less accurate. Compared to the above-presented methods, the proposed method for f_{nadir} prediction in this paper takes into account all of the most important segments such as: i) turbine governor controls, ii) multi-machine power system iii) real-time calculation during the disturbance event and in combination improves on the drawbacks of above presented methods inherently have.

Furthermore methods presented in papers [14]–[16] dynamically adjust UFLS stages thresholds in real-time. In [14], the UFLS thresholds are dynamically changed according to the estimation of f_{nadir} but fails to estimate f_{nadir} in the case of several UFLS stages activation. The interesting method for real-time adjusting UFLS settings is proposed in [15] and [16] which is based on a single-step shedding. However, the single-step load shedding methods are less effective compared to multi-step load shedding regarding the amount of total load capacity to be shed and its ability to withstand larger disturbances. Again, compared to above presented methods, the UFLS algorithm proposed in this paper is based on a multi-step load shedding principles and uses f_{nadir} estimation method which is able to estimate f_{nadir} in cases of multiple UFLS stages activation.

Promising state-of-the-art methods for designing adaptive UFLS protection schemes are based on ROCOF. The ROCOF parameter is mainly used to estimate the generation power deficit and correspondingly determine the precise amount of load to be shed. The paper [17] introduces an effective technique for LOG event estimation by using local ROCOF measurements. The traditional multistage UFLS design improved by incorporating the ROCOF relays signal of distributed generators is presented in [18]. The method is probability-based, and its capability was verified on Iran national grid. In addition to the use of ROCOF, a rate of change of frequency of loads (ROCOFL) indicator can also be used to determine the required amount of load to be shed. Such an approach is presented in [19, 20]. The application of the ROCOF relay signal can also be used not only to determine the required amount of load to be shed but also as a parameter of the decision whether to activate the UFLS as it was shown in [21]. The idea of defining UFLS thresholds, not solely depending on the frequency deviation from the nominal value, but depending on the ROCOF value, was proposed in [22]. The method allows a more effective and faster UFLS response and adaptability which is of great importance for modern EPS with reduced inertia. Although the UFLS ROCOF-based methods presented above have proven to be effective, the main common drawback is their need for an accurate and credible ROCOF value measurement. Due to the synchronous generator swinging, the measured ROCOF values can vary greatly depending on the measurement window. Contrary to those methods, this paper proposes a method which is not dependent on the ROCOF measurements but only uses the information of the activation of generator's ROCOF relay, i.e., the values 1 and 0 as an indicator of whether the ROCOF relay was activated.

1.2. Contribution

Based on the literature survey provided, this paper aims to cover the main drawbacks of the mentioned state-of-the-art literature which can be summarized in the following key points:

- Disregard of turbine governor controls;
- Usage of single-machine power system model;
- Off-line adaptation of setting thresholds and disability to adapt during the disturbance event;
- Usage of single-step load shedding principles;
- f_{nadir} estimation method which is unable to accurately estimate f_{nadir} in cases of multiple UFLS stages activation;
- Requirement for an accurate and credible ROCOF value measurement.

Therefore, the contributions of this paper that improve on the drawbacks identified in currently available proposals of adaptive UFLS methods are as follows:

- Design of a novel UFLS scheme based on multi-machine model with inclusion of turbine governor reaction with adaptive thresholds for avoiding unnecessary activation of particular UFLS stages;
- Design of a UFLS scheme based on real-time prediction method of f_{nadir} which is able to predict f_{nadir} taking into account multiple UFLS stages activations;
- Independence from ROCOF measurements and can be applied to the multi-machine power system model consisting of various types of generating units.

This paper is an extension of the paper published at the MEDPOWER2020 conference [23] and is structured as follows: section II provides a description of proposed adaptive UFLS; section III describes the power system model on which the method effectiveness was tested; the results are presented in section IV and conclusions are given in section V.

2. Proposed design of dynamic adaptive UFLS protection

The need to activate UFLS usually arises in the case of large disturbance like significant loss of generation (LOG) event. This paper proposes adaptive UFLS based on the combination of the generator ROCOF relay activation signal (binary signal: 0 or 1) and the frequency nadir estimation. The ROCOF relay signal is used to provide information about LOG event or transmission line outage event and the frequency nadir estimation is used to obtain information on possible UFLS activation and readjustment of UFLS stages. The main idea is to adjust the UFLS relay settings in order to allow their reaction before the frequency can significantly drop to levels threatening cascading blackouts. In the following chapter, the implementation of the proposed adaptive UFLS scheme is explained in detail.

2.1. Frequency nadir estimation

The method for frequency nadir estimation was adopted from previous work of authors [24] and adjusted for the particular application proposed in this paper. In brief, the method from [24] is based on the

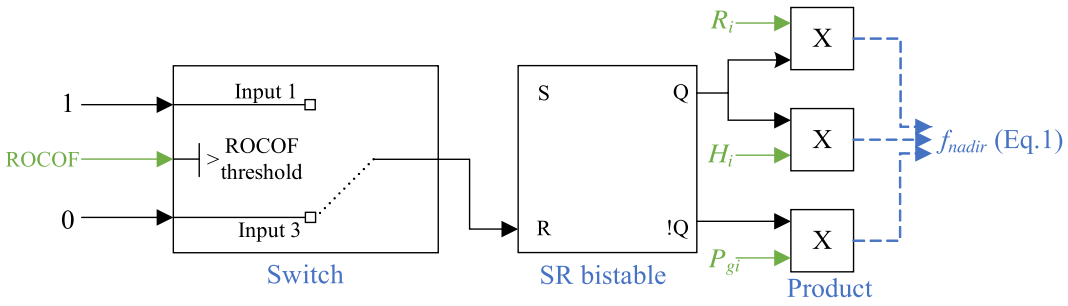

Fig 1. The block scheme of ROCOF relay signal utilization.

system frequency response parabolic approximation. The minimum value of the developed parabolic function approximates the exact frequency nadir value. The method is proven to be very effective, simple, and accurate. The advantage of the developed parabolic approximation method is its capability to be applied to the multi-machine power system and its utilization of the full-order turbine models, while at the same time maintaining quick calculation capability.

The goal of the frequency nadir estimation algorithm is to obtain the frequency nadir f_{nadir} as a function F depending on the LOG size P_{log}, total load amount to be shed P_{UFLS}, i^{th} generator's inertia constant H_i, and i^{th} generator's droop constant R_i:

$$f_{nadir} = F\left(R_1, R_2, \ldots R_i, H_1, H_2, \ldots H_i, P_{log}, P_{UFLS}\right) \tag{1}$$

The f_{nadir} function is given in its polynomial form, but the explicit expression of the function will not be written here, for the sake of simplicity, because it consists of several hundred coefficients for the power system consisting of 10 power plants. The parameters H_i and R_i are assumed to be known for each power plant, while the parameter P_{log} is obtained using the ROCOF relay signal.

However, the method for the f_{nadir} approximation developed in [24] does not consider the case of the UFLS event occurrence. The papers [25,26] provide an analytical approach for determining f_{nadir} considering UFLS settings. The proposed methods are only applicable to the single-machine power systems with low-order turbine models. To develop the f_{nadir} prediction method considering UFLS settings and applicable to the multi-machine power system with full-order turbine models, the method from [24] was extended by adding the following factors expressed in Eq. (2):

$$P(t)_{UFLS} = \sum_{n=1}^{k} P_{UFLS\ n^{th}stage} \cdot u\left(t - x_{UFLS\ n^{th}stage}\right)\# \tag{2}$$

where $P(t)_{UFLS}$ is the activated power (disconnected load power) as a function of time (t), $P_{UFLS\ n^{th}stage}$ is a load to be shed in a particular UFLS stage, k is a total number of the UFLS stage, $x_{UFLS\ n^{th}stage}$ represents a moment in time when the n^{th} UFLS stage activates, $u(t)$ is Heaviside step function defined as in Eq. (3):

$$u(t) = \begin{cases} 0, & t < 0 \\ 1, & t \geq 0 \end{cases} \tag{3}$$

The value of $x_{UFLS\ n^{th}stage}$ is not uniquely determined, but a rather very precise approximation of the value that can be obtained based on the initial ROCOF measurement. The justification for this is that UFLS activation will only occur in the case of very large disturbances which will cause a rapid frequency drop, for example around 1 Hz/s. In this case, UFLS activation occurs before production units could contribute significantly by injecting additional power and thus potentially reduce the initial ROCOF. Therefore, x will mainly be affected by ROCOF and can be determined by Eq.(4):

$$x_{UFLS\ 1.\ stage} = \frac{f_n - f_{ULFS\ 1.stage}}{\frac{P_{log}}{2 \cdot H_{sys}} \cdot f_n} \tag{4}$$

where f_n is the nominal frequency, $f_{UFLS\ 1.stage}$ is the frequency at which UFLS 1st stage activates, H_{sys} is the average system inertia and can be calculated as shown in Eq. (5):

$$H_{sys} = \frac{\sum_{i=1}^{n} S_i H_i}{\sum_{i=1}^{n} S_i} \tag{5}$$

where S_i is the nominal power of the i^{th} generator. Note that the denominator of Eq. (4) is the ROCOF. In addition, the approximation errors are small because x is approximated in a very short time interval. To calculate x for the 2nd UFLS stage, the next equation (Eq. (6)) is applied:

$$x_{UFLS\ 2.\ stage} = (\text{Eq. } 4) + \frac{f_{ULFS\ 1.stage} - f_{ULFS\ 2.stage}}{\frac{P_{log} - P_{UFLS\ 1.stage}}{2 \times H_{sys}} \times f_n} \tag{6}$$

where $f_{UFLS\ 2.stage}$ is the frequency at which UFLS 2nd stage activates, $P_{UFLS\ 1.stage}$ is the amount of the load that was to be shed in the 1st stage. The expressions for the remaining UFLS stages can be calculated analogously. It should be noted that the values, i.e., the time obtained for x as a moment of activation for the third, fourth, and fifth UFLS stages are likely to be less than the actual values because in those moments the power plant's contributions become more significant. This can be considered as an analysis of the marginal (best) case, that is, if the model shows that there will be an activation of, e.g., UFLS 3rd stage, then it would actually occur in the real power system. In addition, a small difference between the actual value of f_{nadir} and the one calculated by Eq. (1) may exist because Eq. (1) does not consider the limitation of the primary power reserve of the individual power plant.

2.2. Utilization of ROCOF relay signal

The main purpose of the usage of ROCOF relay signal, once the relay activation occurs i.e., due to power plant tripping, is to send a binary signal to set the real value for P_{log} in (1). Furthermore, the purpose of ROCOF relay signal is to set value "0″ for the corresponding parameters H_i and R_i in (1) that are related to particular production unit. The block implementation is shown in Fig. 1.

The switch block passes the signal through the input signal 3 as long as the ROCOF value is below the set threshold. The function of the SR bistable block is to hold output signal after the power plant tripping. Initial condition (state of Q) is set to 1. The parameter P_{gi} in Fig. 1 represents the current power plant production and is defined in Eq. (7) where n is the total number of power plants in the observed system.

$$P_{log} = \sum_{i=1}^{n} P_{gi} \tag{7}$$

2.3. Dynamically adaptive UFLS block scheme

The dynamic adaptive UFLS block scheme proposed in this paper is capable of adjusting the frequency thresholds of the various UFLS stages according to the estimated frequency nadir which is by itself changed in accordance to the actual activation of different stages. When a power

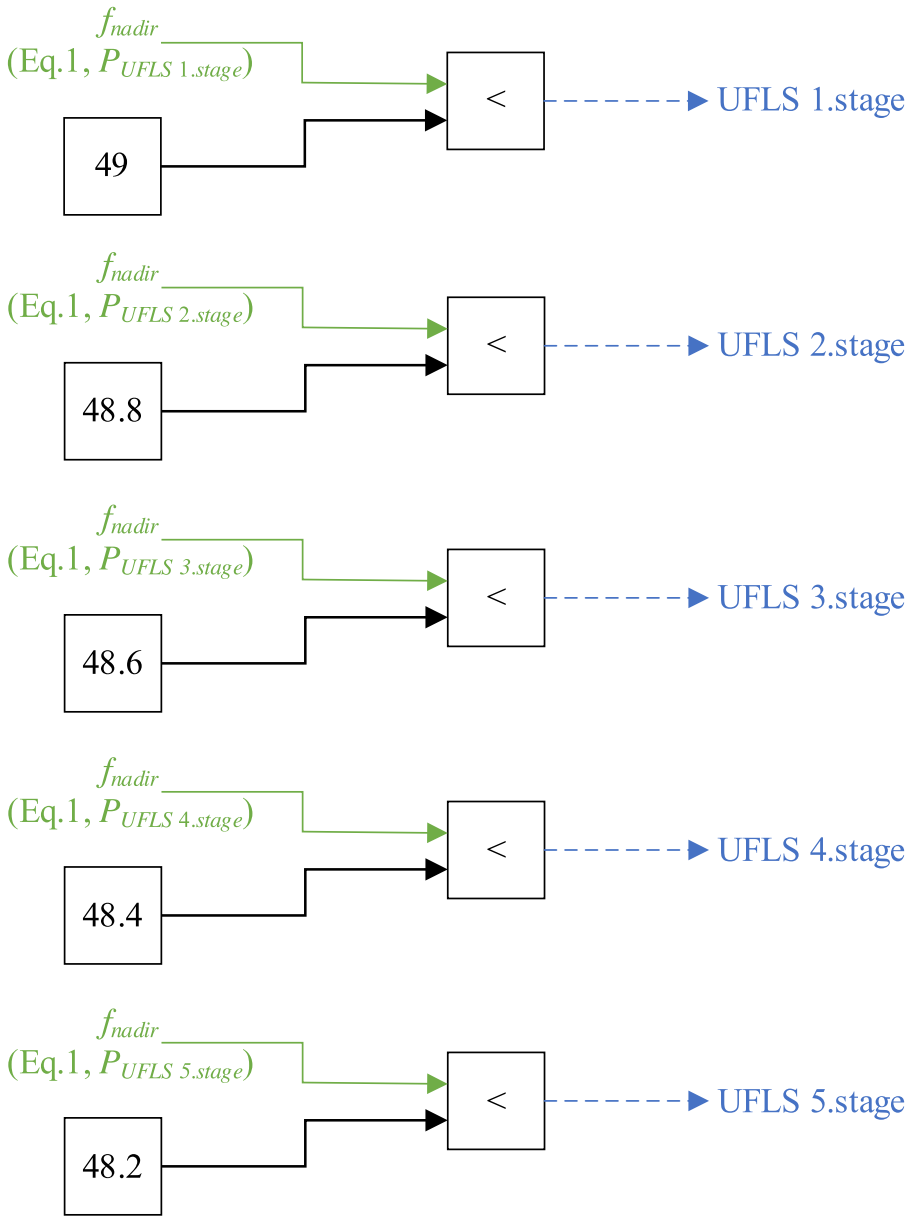

Fig. 2. The decision-making block of the proposed algorithm.

Table I
UFLS settings of the Croatian EPS.

UFLS stage	Frequency [Hz]	Load-shedding [%]	Total load-shedding [%]
1. stage	49.00	5	5
2. stage	48.80	10	15
3. stage	48.60	10	25
4. stage	48.40	10	35
5. stage	48.20	10	45
6. stage	48.00	5	50

plant trip occurs, Eq. (1) estimates the f_{nadir} value according to the disturbance expressed as P_{log} size. If in this way calculated f_{nadir} value is between, for example, the 2nd and 3rd UFLS threshold stages, the algorithm increases the thresholds for the first and second UFLS stages to react earlier to potentially avoid activating also the third UFLS stage, thus reducing the total load shed amount. To consider the percentage of load shedding, while estimating f_{nadir} value in the case ULFS is activated, the parameter $P(t)_{UFLS}$ from Eq. (2) was added to the Eq. (1). This value provides an insight into the expected f_{nadir} and how many UFLS stages are expected to be activated. To determine at which UFLS stage the threshold should be increased, the decision-making block was developed and is shown in Fig. 2. The output of the relational operator 'less than' in Fig. 2 can be either 0 or 1. The decision-making block parameters were modified according to the actual UFLS settings in the Croatian electric power system which are shown in Table I. According to Fig. 2, if the f_{nadir} value is anticipated to be higher than 49.00 Hz, the UFLS settings remain as in the conventional scheme (Table I). However, if the f_{nadir} value falls below 49.00 Hz, then the decision-making block determines which thresholds should be increased.

To increase the UFLS threshold settings for an incremental step factor, an additional block performing that action was developed. This function block is shown on Fig. 3. The increment step factor can be set to the arbitrarily value, but in this case, it is set to be 0.2 Hz. Generally, the larger the increment step, the greater the contribution of the proposed UFLS scheme. Fig. 3 shows only the UFLS 1st stage, while for other UFLS stages, the parameters UFLS threshold, the increment step, and the amount of load to be shed should be changed according to the desired

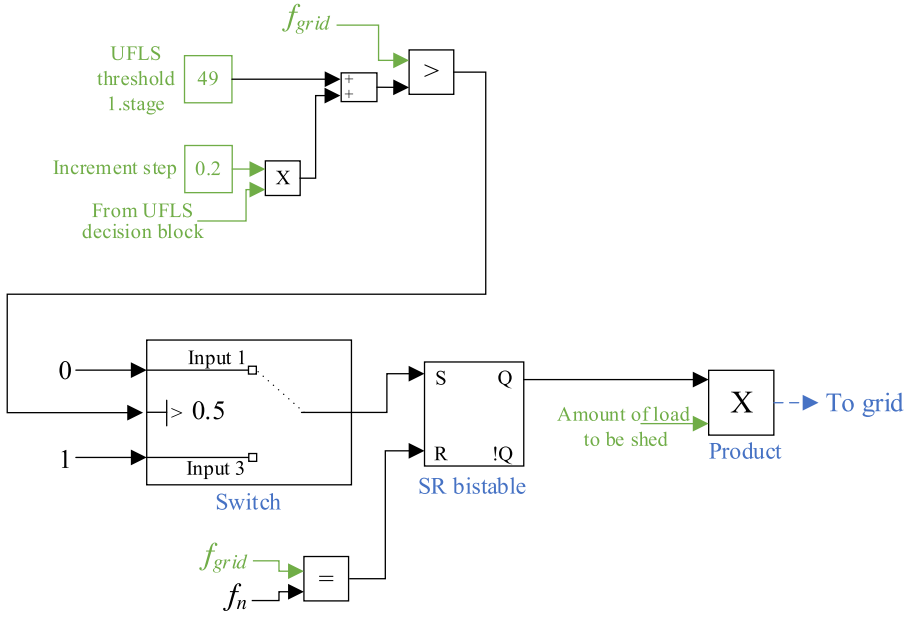

Fig. 3. Function block designed to increase of the UFLS thresholds.

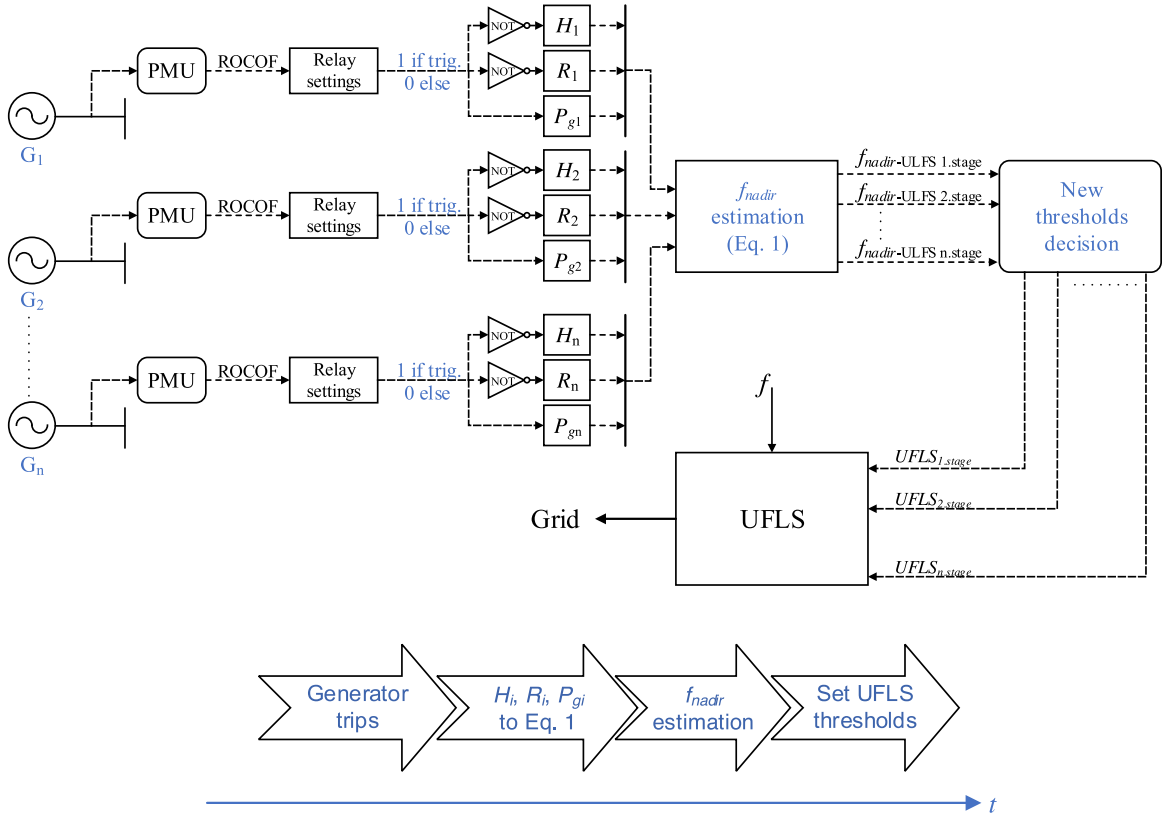

Fig. 4. Dynamic adaptive UFLS protection model.

UFLS settings.

When the frequency falls below the UFLS threshold, the output of the relational operator 'greater than' sends the value "0" to the switch block which then passes the signal through the input 3 and the value "1" is set to S input of the SR bistable block. In that way, the UFLS stage is activated. The function is reset when the frequency returns to the nominal value.

The advantage of the proposed method is that it provides the system with the same or greater response compared to the conventional UFLS method. In other words, if the proposed method is not activated, the same contribution is retained similar to the conventional UFLS method, while if the proposed method activates, then a higher contribution is provided to the system in the initial stages and therefore activations of further UFLS stages could be avoided and total load shed can be reduced.

The measurement and communication delays in the system can reduce the efficiency of the algorithm if the input data is not accessible

Table II
Power plants parameters.

Parameters	HPP1	HPP2	HPP3	HPP4	HPP5	HPP6	$TPP_{rt}1$	$TPP_{rt}2$	$TPP_{rt}3$	TPP_{nrt}
Nominal power	100 MW	150 MW	200 MW	200 MW	250 MW	300 MW	100 MW	200 MW	300 MW	200 MW
Inertia constant H	3.5	4	3	5 s	5 s	4 s	6 s	5	6	5
Droop $R_{H,T}$	4%	6%	5%	5%	5%	4%	5%	6%	5%	4%
Governor time constant T_G	0.2s	0.25s	0.3s	0.2 s	0.3 s	0.25 s	0.2 s	0.25	0.3	0.25
Reset time T_R	5	5.5	6	6 s	6.5 s	7 s	–	–	–	–
Transient droop R_T	0.4	0.45	0.35	0.5 s	0.4 s	0.45 s	–	–	–	–
Turbine time constant T_W	0.95	1	1.05	1.05 s	1.10 s	1.00 s	–	–	–	–
Reheater time constant T_{RH}	–	–	–	–	–	–	7 s	6	8	–
Control valve time constant T_{CH}	–	–	–	–	–	–	0.25 s	0.3	0.35	0.3
Fraction of the power in the high-pressure steam turbine F_{HP}	–	–	–	–	–	–	0.35	0.3	0.35	–

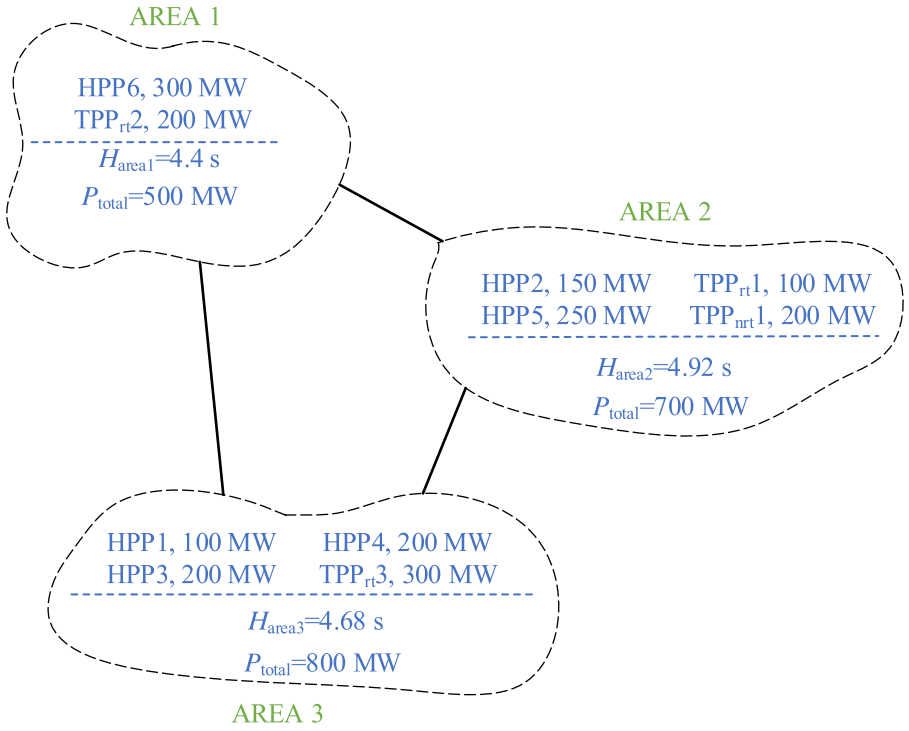

Fig. 5. The power system model.

before the frequency reaches the value at which UFLS Stage 1 activates. However, the time required for UFLS to activate varies from system to system but is generally greater than one second as shown by the 2016 South Australia Blackout [27] or 2019 UK Blackout case [28]. The paper [29] shows that the delays in using PMU associated with various communication links are estimated to be 100 ms - 300 ms. Therefore, delays averaging 200 ms do not significantly affect the proper operation of the proposed algorithm.

The complete dynamically adaptive UFLS protection model is shown in Fig. 4. It should be noted that the PMUs are owned by the TSO, while the ROCOF relays are part of the power plant, but with their cooperation, the scheme in Fig. 4 could be realized.

3. Power system model

The method effectiveness is tested on a multi-machine power system model. The power system consists of 10 power plants: 6 hydropower plants, 3 thermal power plants with a reheat steam turbine, and 1 thermal power plant with a non-reheat turbine. The total capacity of the modelled system is 2 GW. Generating units are represented with the full-order turbine models [30]. Hydropower generating unit turbine model is represented by Eq. (8). Thermal generating unit with a reheat turbine model is represented by Eq. (9) and thermal generating unit with a non-reheat turbine model by Eq. (10).

$$\mathrm{HPP}(s) = \frac{1}{R_H}\frac{1}{1+sT_G}\frac{1+sT_R}{1+s\left(\frac{R_T}{R_H}\right)T_R}\frac{1-sT_W}{1+0.5sT_W} \tag{8}$$

$$TPP_{rt}(s) = \frac{1}{R_T}\frac{1}{1+sT_G}\frac{1+sF_{HP}T_{RH}}{(1+sT_{CH})(1+sT_{RH})} \tag{9}$$

$$TPP_{nrt}(s) = \frac{1}{R_T}\frac{1}{1+sT_{CH}} \tag{10}$$

All relevant power plants parameters are given in Table II for each generating unit.

As the initial ROCOF directly depends on the amount of inertia in a certain area, the power system is divided into 3 areas. The areas differ in total generation capacity as well as in the amount of inertia as shown on Fig. 5. The inertia constant for each area shown in Fig. 5 is calculated according to the base capacity of the corresponding area. Despite the uncertainty associated with the production from RES, the proposed algorithm works regardless of the number and type of production units,

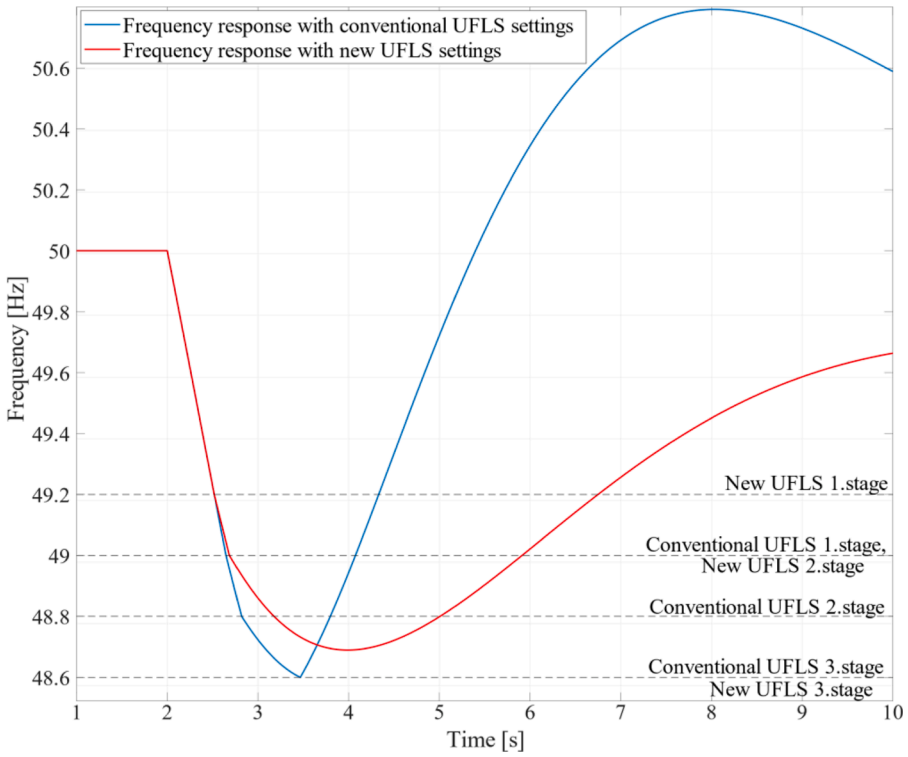

Fig. 6. Comparison of conventional UFLS and proposed adaptive UFLS.

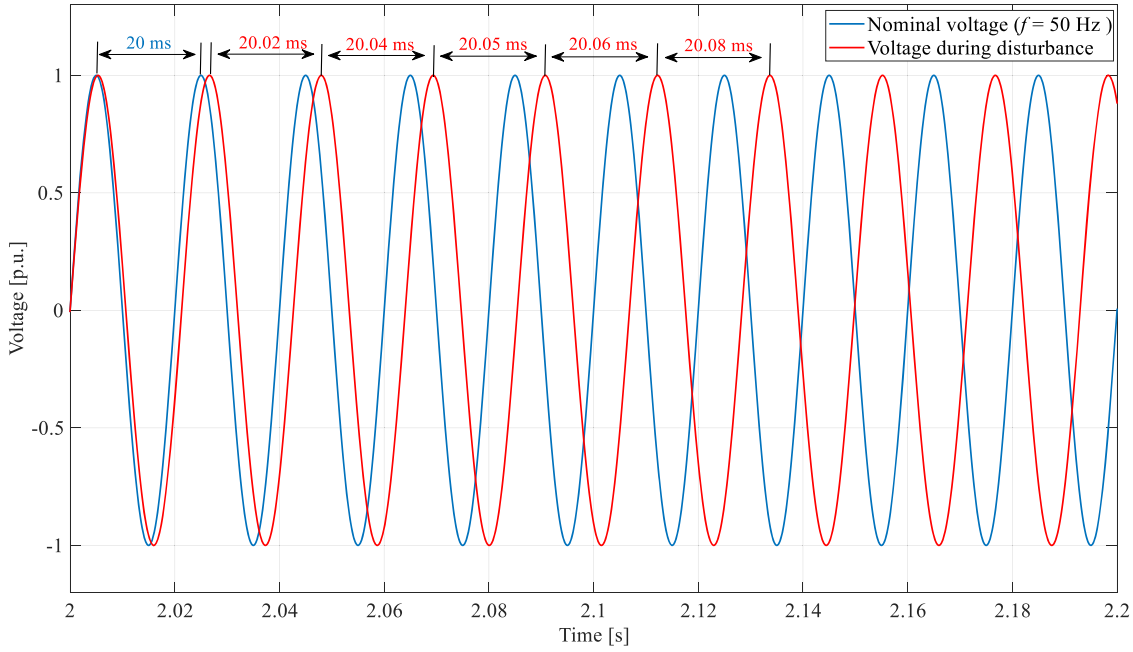

Fig. 7. The comparison of the nominal voltage waveform and voltage waveform during a disturbance.

including RES, in operation at any given moment. RES that are able to provide a virtual response would be modelled by a convenient transfer function, usually with a small time constant. In addition, if WPPs are present in the system, the value of their inertia constant is simply added to the algorithm just as it is done for synchronous generators. Besides, the system inertia can be monitored and measured in real-time as it is presented in [31]. Due to the difference in the inertia constants of individual areas and the disturbance propagation, the ROCOF values in individual areas differ. It primarily depends on the fault location, so it is possible to simulate the case in which only a subset of all power plants trips due to the activation of ROCOF relays, while the power plants in other segments of the system remain connected to the network because their ROCOF relays did not detect ROCOF higher than the set threshold. The paper [32] shows that the ROCOF value in one area can be 2–3 times higher than the measured ROCOF value in other areas within the same power system.

Table III
UFLS model parameters.

Parameter	Adaptive UFLS system	Model measured value
$x_{UFLS\ 1.stage}$	0.657 s	0.649 s
$x_{UFLS\ 2.stage}$	0.827 s	0.820 s
f_{nadir} (UFLS 1.stage)	47.53 Hz	47.50 Hz
f_{nadir} (UFLS 1. stage+2.stage)	48.62 Hz	48.57 Hz
f_{nadir} (UFLS 1.stage+2.stage+3.stage)	48.88 Hz	Not activated

4. Results

To show the advantages of the proposed dynamically adaptable UFLS method compared to the conventional methods, simulation tests were performed. A case was simulated in which two power plants from area 2, i.e. HPP5 and TPP_{nrt}, trip due to the ROCOF relay activation. It was assumed that the power plants were operating at rated power, so there was a power deficit of 0.225 p.u. (450 MW) created in the system as a result of this outage. In the power system with the conventional UFLS settings (Table I), the frequency drop would be stopped at 48.60 Hz which means that three stages of UFLS would be activated for this LOG event. However, if the proposed adaptive UFLS is implemented in the system, with appropriate algorithm decisions of adjusting settings of particular UFLS stages, 3rd UFLS stage activation was successfully avoided as is shown in Fig. 6.

Fig. 6 also shows the improved functionality of the algorithm in a manner that it precisely recognized that it was only necessary to raise the thresholds for the 1st and 2nd UFLS stages, while the threshold for the 3rd UFLS stage remained unchanged. The thresholds were raised by the increment step of 0.2 Hz, so this is the reason why in Fig. 6 the conventional UFLS 1st stage and new UFLS 2nd stage match. In addition, looking at the frequency response with the conventional UFLS algorithm (blue line on Fig. 6), the great frequency overshoot, that occurred after the activation of the 3rd UFLS stage, is observed. This is one of the very common problems of conventional UFLS schemes. If too much load is shed, the UFLS operation can actually worsen the frequency stability. The reason for the occurrence of frequency overshoot lies in the fact that after UFLS 3. stage activation took place, a great power surplus appeared in the system. It is evident how important it is to avoid unnecessary activations of individual UFLS stages since the backfire consequences also need to be considered.

More details on the characteristics of the overall control system of the proposed adaptive UFLS are given in Table III. It can be seen that the moments in which the 1st and 2nd UFLS stages are activated were very precisely calculated. The deviation from the model measured values is less than 10 milliseconds. Furthermore, the developed approximation of f_{nadir} also shows great accuracy. For clarity, the value f_{nadir} (UFLS 1.stage) in Table III shows the f_{nadir} in the case of UFLS 1.stage activation only. The deviation is less than 50 mHz which is insignificant for the functionality of the proposed UFLS algorithm. Note that the value of f_{nadir} anticipated by Eq. (1) considering UFLS 3rd stage is meaningless, because if the UFLS 3rd stage activation occurs, then the minimum frequency value is at least equal to the threshold value of that UFLS stage. In this case, it should be set at the value of at least 48.60 Hz. The reason for this can be found in the fact that frequency fall was actually stopped at the value above the set threshold of UFLS 3rd stage.

In addition, Fig. 7 shows the change in voltage waveform as a result of the frequency drop. Assuming that the value of the voltage magnitude is constant (V_0=1 p.u.) during the disturbance, the main difference is manifested in the increase of the sine wave period in proportion to the frequency deviation from the nominal value.

5. Conclusion

In this paper, a new dynamically adaptive UFLS protection scheme algorithm was proposed. The method is based on the dynamic adaptive reconfiguration of conventional UFLS strategies. By combining real-time information on the generator's states, turbine-governor parameters, and frequency nadir estimation, the effectiveness of the UFLS function is significantly improved. The approach focuses on the usage of the data about the generator current power, inertia constant and droop constant that are used by the algorithm to estimates the frequency nadir in the case of LOG event. Given the state of the system and the estimated frequency nadir, the algorithm adjusts the UFLS relay settings and stages thresholds. The main advantage of the proposed algorithm is that the required number of UFLS stages to be activated is reduced compared to the conventional strategies. The algorithm is capable of deciding when and what UFLS relay stages setting need to be adjusted to avoid activating further UFLS stages and avoid further load shedding. The functionality of the proposed method was tested on a multi-machine power system consisting of various generation technologies. The tests showed that the proposed ULFS method activates a smaller number of stages compared to the conventional ULFS strategies. This means that the system generally sheds a smaller part of consumers, approximately around 5–10% of consumption, depending on the UFLS relay settings and thus greatly reducing potentially associated costs and increasing the overall social welfare.

CRediT authorship contribution statement

Tomislav Baškarad: Conceptualization, Methodology, Software, Validation, Writing – original draft, Writing – review & editing, Formal analysis. **Ninoslav Holjevac:** Conceptualization, Data curation, Writing – original draft, Writing – review & editing, Supervision. **Igor Kuzle:** Investigation, Writing – review & editing. **Igor Ivanković:** Validation, Writing – review & editing.

Declaration of Competing Interest

The authors declare that they have no known competing financial interests or personal relationships that could have appeared to influence the work reported in this paper.

Acknowledgements

This work was funded by the European Union and is a part of the H2020 project "CROSSBOW - CROSS Border management of variable renewable energies and storage units enabling a transnational Wholesale market" (Grant No. 77343) and through the European Regional Development Fund Operational Programme Competitiveness and Cohesion 2014–2020 of the Republic of Croatia under project KK.01.1.1.04.0034 "Connected Stationary Battery Energy Storage". This document has been produced with the financial assistance of the European Union. The contents of this document are the sole responsibility of authors and can under no circumstances be regarded as reflecting the position of the European Union.

References

[1] D. Zografos, M. Ghandhari, R. Eriksson, Power system inertia estimation: utilization of frequency and voltage response after a disturbance, Electr. Power Syst. Res. 161 (Aug. 2018) 52–60.
[2] Y.R. O.mar, I.Z. A.bidin, S. Yusof, H. Hashim, H.A. A.bdul Rashid, Under frequency load shedding (UFLS): principles and implementation, in: PECon2010 - 2010 IEEE International Conference on Power and Energy, 2010, pp. 414–419.
[3] K.S. R.atnam, K. Palanisamy, G. Yang, Future low-inertia power systems: requirements, issues, and solutions - A review, Renewable and Sustainable Energy Rev. 124 (01-May-2020), 109773.
[4] P.S. W.right, P.N. D.avis, K. Johnstone, G. Rietveld, A.J. R.oscoe, Field measurement of frequency and ROCOF in the presence of phase steps, IEEE Trans. Instrum. Meas. 68 (6) (Jun. 2019) 1688–1695.
[5] J. Riesz, J. Palermo, International review of frequency control adaptation, Report, Australian Energy Mark. Operator (2016).
[6] I. Ivankovic, I. Kuzle, N. Holjevac, Dynamic angle instability simulation framework based on reference model platform, Proceedings - 2018 IEEE Int. Conference on

Environ. Electrical Eng. 2018 IEEE Ind. Commercial Power Syst. Eur. EEEIC/I and CPS Eur. (2018) 2018.
[7] H. Haes Alhelou, M.E. H.amedani Golshan, T.C. N.jenda, N.D. H.atziargyriou, An overview of UFLS in conventional, modern, and future smart power systems: challenges and opportunities, in: Electric Power Systems Research, 179, Elsevier Ltd, 01-Feb-2020, 106054.
[8] M. Larsson, C. Rehtanz, Predictive frequency stability control based on wide-area phasor measurements, Proceedings of the IEEE Power Eng. Society Trans. Distribution Conference 1 (2002) 233–238. SUMMER.
[9] A. Ketabi, M. Hajiakbari Fini, Adaptive underfrequency load shedding using particle swarm optimization algorithm, J. Appl. Res. Technol. 15 (1) (Feb. 2017) 54–60.
[10] U. Rudez, R. Mihalic, Predictive underfrequency load shedding scheme for islanded power systems with renewable generation, Electr. Power Syst. Res. 126 (May 2015) 21–28.
[11] Q. Walger, Y. Zuo, A. Derviškadić, G. Frigo, M. Paolone, OPF-based under frequency load shedding predicting the dynamic frequency trajectory, Electr. Power Syst. Res. 189 (Dec. 2020), 106748.
[12] S.S. B.anijamali, T. Amraee, Semi-Adaptive setting of under frequency load shedding relays considering credible generation outage scenarios, IEEE Trans. Power Deliv. 34 (3) (Jun. 2019) 1098–1108.
[13] M. Lukic, I. Kuzle, S. Tesnjak, Adaptive approach to setting underfrequency load shedding relays for an isolated power system with private generation, Proceedings of the Mediterranean Electrotechnical Conference - MELECON 2 (1998) 1122–1125.
[14] B. Potel, V. Debusschere, F. Cadoux, U. Rudez, A real-time adjustment of conventional under-frequency load shedding thresholds, IEEE Trans. Power Deliv. 34 (6) (Dec. 2019) 2272–2274.
[15] A.Q. S.antos, R.M. M.onaro, D.V. C.oury, M. Oleskovicz, A new real-time multi-agent system for under frequency load shedding in a smart grid context, Electr. Power Syst. Res. 174 (Sep. 2019), 105851.
[16] M.A. K.abir, A.H. C.howdhury, N. Al Masood, A dynamic-adaptive load shedding methodology to improve frequency resilience of power systems, Int. J. Electr. Power Energy Syst. 122 (Nov. 2020), 106169.
[17] M. Sun, G. Liu, M. Popov, V. Terzija, S. Azizi, Underfrequency load shedding using locally estimated ROCOF of the center of inertia, IEEE Trans. Power Syst. (2021).
[18] T. Amraee, M.G. D.arebaghi, A. Soroudi, A. Keane, Probabilistic under frequency load shedding considering ROCOF Relays of distributed generators, IEEE Trans. Power Syst. 33 (4) (Jul. 2018) 3587–3598.
[19] A. Mokari-Bolhasan, H. Seyedi, B. Mohammadi-Ivatloo, S. Abapour, S. Ghasemzadeh, Modified centralized ROCOF based load shedding scheme in an islanded distribution network, Int. J. Electr. Power Energy Syst. 62 (Nov. 2014) 806–815.
[20] M. Marzband, M.M. M.oghaddam, M.F. A.korede, G. Khomeyrani, Adaptive load shedding scheme for frequency stability enhancement in microgrids, Electr. Power Syst. Res. 140 (Nov. 2016) 78–86.
[21] L. Sigrist, A UFLS scheme for small isolated power systems using rate-of-change of frequency, IEEE Trans. Power Syst. 30 (4) (Jul. 2015) 2192–2193.
[22] Y. Zuo, G. Frigo, A. Derviškadić, M. Paolone, Impact of synchrophasor estimation algorithms in ROCOF-based under-frequency load-shedding, IEEE Trans. Power Syst. 35 (2) (Mar. 2020) 1305–1316.
[23] T. Baškarad, N. Holjevac, I. Kuzle, I. Ivanković, N. Zovko, ROCOF importance in electric power systems with high renewables share: a simulation case for Croatia, Mediterranean Conference on Power Generation, Transmission, Distribution and Energy Conversion (MEDPOWER), Cyprus (2020) 1–10.
[24] T. Baskarad, I. Kuzle, N. Holjevac, Photovoltaic system power reserve determination using parabolic approximation of frequency response, IEEE Trans. Smart Grid (2021) 1.
[25] C. Li, et al., Continuous under-frequency load shedding scheme for power system adaptive frequency control, IEEE Trans. Power Syst. 35 (2) (Mar. 2020) 950–961.
[26] T. Shekari, F. Aminifar, M. Sanaye-Pasand, An analytical adaptive load shedding scheme against severe combinational disturbances, IEEE Trans. Power Syst. 31 (5) (Sep. 2016) 4135–4143.
[27] R. Yan, N. -Masood, T. Kumar Saha, F. Bai and H. Gu, "The anatomy of the 2016 South Australia blackout: a catastrophic event in a high renewable network," in IEEE Trans. Power Syst., vol. 33, no. 5, pp. 5374–5388, Sept. 2018, doi: 10.1109/TPWRS.2018.2820150.
[28] National Grid ESO, "Technical Report on the events of 9 August 2019", September 2019, available at: https://www.nationalgrideso.com/document/152346/download.
[29] B. Naduvathuparambil, M.C. V.alenti, A. Feliachi, Communication delays in wide area measurement systems, Proceedings of the Thirty-Fourth Southeastern Symposium on Syst. Theory (Cat. No.02EX540) (2002), https://doi.org/10.1109/SSST.2002.1027017, 118–122.
[30] P.(Prabha) Kundur, N.J. B.alu, M.G. L.auby, Power System Stability and Control, McGraw-Hill, 1994.
[31] K. Tuttelberg, J. Kilter, D. Wilson, K. Uhlen, Estimation of power system inertia from ambient wide area measurements, IEEE Trans. Power Systems 33 (6) (Nov. 2018) 7249–7257, https://doi.org/10.1109/TPWRS.2018.2843381.
[32] J. Đaković, M. Krpan, P. Ilak, T. Baškarad, I. Kuzle, Impact of wind capacity share, allocation of inertia and grid configuration on transient ROCOF: the case of the Croatian power system, Int. J. Electr. Power Energy Syst. 121 (Oct. 2020), 106075.